Biosensors and Bioelectronics 59 (2014) 328–334

Contents lists available at ScienceDirect

Biosensors and Bioelectronics

journal homepage: www.elsevier.com/locate/bios

Ultrasensitive detection of deltamethrin by immune magnetic nanoparticles separation coupled with surface plasmon resonance sensor

Xia Liu [a,b,*], Lei Li [a], You-Qian Liu [a], Xing-Bo Shi [a], Wen-Jin Li [a], Yang Yang [a], Lu-Gang Mao [a]

[a] College of Food Science and Technology, Hunan Agricultural University, Hunan Province Key Laboratory of Food Science and Biotechnology, Changsha 410128, PR China

[b] State Key Laboratory of Chemo/Biosensing and Chemometrics, Hunan University, Changsha 410082, PR China

ARTICLE INFO

Article history:
Received 29 November 2013
Received in revised form
28 February 2014
Accepted 11 March 2014
Available online 13 April 2014

Keywords:
Surface plasmon resonance sensor
Fe_3O_4 magnetic nanoparticles
Deltamethrin detection

ABSTRACT

Small molecules or analytes present in trace level are difficult to be detected directly using conventional surface plasmon resonance (SPR) sensor, due to its small changes in the refractive index induced by the binding of these analytes on the sensor surface. In this paper, a new approach that combines SPR sensor technology with Fe_3O_4 magnetic nanoparticles (MNPs) assays is developed for directly detecting of deltamethrin in soybean. The Fe_3O_4 MNPs conjugated with antibodies specific to antigen serves as both labels for enhancing refractive index change due to the capture of target analyte, and "vehicles" for the rapid delivery of analyte from a sample solution to the sensor surface. Meanwhile, SPR direct detection format without Fe_3O_4 MNPs and gas chromatography (GC) analysis were conducted for detection of deltamethrin in soybean to demonstrate the amplification effect of Fe_3O_4 MNPs. A good linear relationship was obtained between SPR responses and deltamethrin concentrations over a range of 0.01–1 ng/mL with the lowest measurable concentration of 0.01 ng/mL. The results reveal that the detection sensitivity for deltamethrin was improved by 4 orders of magnitude compared with SPR direct detection format. The recovery of 95.5–119.8% was obtained in soybean. The excellent selectivity of the present biosensor is also confirmed by two kinds of pesticides (fenvalerate and atrazine) as controls. This magnetic separation and amplification strategy has great potential for detection of other small analytes in trace level concentration, with high selectivity and sensitivity by altering the target-analyte-capture agent labeled to the carboxyl-coated Fe_3O_4 MNPs.

1. Introduction

As one of the most popular and widely used insecticides in the world (Elliot et al., 1974; Gorge and Nagel, 1990), deltamethrin belongs to the synthetic type II pyrethroid insecticide that kills insects through dermal contact and digestion. There are many uses for deltamethrin from agricultural uses to home pest control. Deltamethrin's popularity originates in its stability and longer residual activity, so residues are commonly found in food, consumer products and the environment (Koprücü and Aydın, 2004). Human exposure to deltamethrin can occur through inhalation, ingestion, and the dermal routes of eye and skin contact, each of those can possibly lead to acute health effects such as choreoathetosis, hyperexcitability, ataxia, dermatitis, diarrhea, tremors, and vomiting (Ray et al., 2000). Deltamethrin is also highly toxic as a neurotoxin to aquatic life, particularly fish (Velíšek et al., 2007). Consequently, it is very important to develop a rapid, high sensitive and specific detection method for monitoring deltamethrin residues in crop, drinking water and soil.

The traditional analytical methods for deltamethrin detection focus on the combination of chromatographic techniques and multiple detection techniques, such as gas chromatography with an electron capture detector (GC-ECD) (Ding et al., 2000) gas chromatography–mass spectrometry (GC–MS) (Esteve-Turrillas et al., 2005), high-performance liquid chromatography-UV detection (HPLC-UV) (Wongsa and Burakham, 2012), high-performance liquid chromatography-diode array detection (HPLC-DA) (Tsochatzis et al., 2010), high-performance liquid chromatography–mass spectrometry (HPLC–MS) (Ferrer et al., 2005), or liquid chromatography combined with postcolumn photochemically induced fluorometry derivatization and fluorescence detection (HPLC-FD) (Vázquez et al., 2008). Although those methods can give reproducible, reliable, accurate and sensitive

* Corresponding author at: College of Food Science and Technology, Hunan Agricultural University, Furong District, Changsha 410128, PR China. Tel.: +86 731 84673517.
E-mail address: liuxiaspr@gmail.com (X. Liu).

http://dx.doi.org/10.1016/j.bios.2014.03.020
0956-5663/

determination results, they need costly apparatus, tedious and complicated multi-step sample preparation, which is time-consuming and ungreen.

With the development of various sensors and their combination with metal nanoparticles (NPs) or quantum dots, currently, the techniques has been progressed from the biomolecule detection to the small molecules detection. For example, sensor has had analytical performance as excellent as HPLC for deltamethrin detection (Ge et al., 2011a, 2011b). Among them, surface plasmon resonance (SPR) sensor, cooperating with nanoparticles as an amplification reagent, has been reported for the detection of small molecules and attracted more and more attention (Chang et al., 2011; Kim et al., 2012; Pelossof et al., 2012; Zamfir et al., 2011; J.L. Wang et al., 2011, Y. Wang et al., 2011). All kinds of NPs, including Au NPs (Urusov et al., 2011), Ag NPs (Vasileva et al., 2011), SiO_2 NPs (Luckarift et al., 2007), Pd NPs (Lin et al., 2008), and Pt NPs (Beccati et al., 2005), had been demonstrated for SPR signal amplification in small molecule detection. Although these methods can enhance effectively the SPR sensitivity enhancement, they usually require more time and complex process for the selective enrichment and separation of target molecules from a sample solution, especially for analytes in complex agriculture products or food matrixes (Liang et al., 2012).

Recently, magnetic nanoparticles (MNPs) have been received increasing attention on application for the immobilization and purification of biomolecules in SPR. There are three reasons for MNPs application in SPR: firstly, MNPs have the large surface area, which allows for a high density of biomolecule immobilization; secondly, MNPs have excellent magnetism, which allows for direct capture, separation, and even concentration of target molecules by external magnetic field (Chen et al., 2008; Heidari et al., 2012); thirdly, MNPs have high refractive index and the high molecular weight, which may effectively increase the SPR signal. These advantages make MNPs act not only as an amplifier to enhancing the sensitivity of the SPR sensor, but also as a concentration purification agent to reduce the background interference of unknown compound in SPR assay. In addition, MNPs are more economical than Au NPs, because of the low cost of Fe salts. So far, several research groups have confirmed superior performance of MNPs and demonstrated promising SPR biosensor applications for biomolecules detection. For example, J.L. Wang et al. (2010, 2011) have developed a novel SPR biosensor for detecting adenosine and thrombin based on indirect competitive inhibition assay and sandwich assay, respectively, using Fe_3O_4 MNP–aptamer conjugates as the amplification reagent. Liang et al. (2012) applied sandwich immunoassay based on the SPR biosensor to detect α-fetoprotein (AFP) by immobilizing a primary AFP antibody on the surface of a-mercapto-1-propanesulfonate/chitosan–ferrocene/Au NP film, employing Fe_3O_4@Au–AFP secondary antibody conjugates as the amplification reagent.

In this work, we report a new approach that combines SPR sensor technique with Fe_3O_4 MNP assay for simple, rapid and ultrasensitive detection of the deltamethrin. Here, the surface of the Fe_3O_4 MNPs was modified by carboxyl groups which make the MNPs be easily functionalized by antibodies. The Fe_3O_4 MNPs conjugated with antibodies simultaneously served as "vehicles" for rapid delivery of target analyte from a sample to the sensor surface, and served as labels increasing the SPR detection sensitivity due to high refractive index and the high molecular weight of Fe_3O_4 MNPs. Accordingly, the direct detection of deltamethrin can be achieved by injecting conjugates of the Fe_3O_4 MNP–anti-deltamethrin monoclonal antibody (Ab) enriched deltamethrin on the SPR sensor surface modified with chitosan (Scheme S1). Moreover, this assay can simplify the pretreatment process of the sample, and increase the detection accuracy of small deltamethrin in complex agriculture product or food matrixes. To demonstrate the usefulness of the approach developed, deltamethrin in soybean samples were analyzed with the SPR sensor, and the performance for deltamethrin analysis on the SPR sensor was further compared with that on SPR direct detection format and GC-ECD method, respectively. This proposed approach can carry out an accurate and ultrasensitive detection for deltamethrin, and also can be used to detect other analytes of interest by altering the corresponding antibody in the MNPs conjugates.

2. Experimental

2.1. Materials and reagents

Ab was obtained from WuHan SanYing Proteintech Group, Inc. Nodium hydroxide (NaOH), anhydrous ether, ethyl acetate, n-hexane and bovine serum albumin (BSA) were obtained from Beijing Dingguo Biotechnology (Beijing, China). Deltamethrin, 3-mercaptopropionic acid (MPA), n-hydroxysuccinimide (NHS), 1-ethyl-3-(3-dimethylaminopropyl) carbodiimide hydrochloride (EDC), mercaptoethylamine (MEA), chitosan (medium molecular weight) and ethanol amine (EA) were purchased from Sigma-Aldrich (St. Louis, MO, USA). All reagents were of analytical grade and used without further purification, and ultrapure water was used throughout this work.

Ab was dissolved with 0.01 M phosphate buffer solution (PBS, pH 7.4), and stored at 4 °C. Deltamethrin was dissolved with anhydrous ethanol as stock solution, and then diluted with PBS as standard solution. Blocking buffer solution was composed of PBS containing 0.1 M EA.

2.2. Apparatus

The SPR measurements were conducted on a BI-SPR 2000 system (Biosensing Instrument Inc., Tempe, AZ). A flow delivery system incorporated in the BI-SPR platform pumped samples onto the SPR sensor chip at a flow rate of 10 μL/min. The bare Au sensor chip was obtained from Biosensing Instrument Inc. Instrument operations and data processing were performed by the BI-SPR 2000 control software (version 2.2.0.). Thoroughly degassed 0.01 M PBS (pH 7.4) buffer was used as the carrier solution. Transmission electron microscope (TEM) was carried out on JSM-6380 (JEOL). The inductively coupled plasma atomic emission spectrometry (ICP) was carried out on optima 8300 (Perkinelmer, USA). The UV–visible spectrum was recorded on UV-2450 ultraviolet–visible spectrophotometer (Shimadu, Japan). The FI-IR spectrum was recorded on Spectrum 65 spectrometer (Perkinelmer, USA).

2.3. The synthesis and biofunctionalization of carboxyl group modified Fe_3O_4 MNPs

The carboxyl group modified Fe_3O_4 MNPs (carboxyl-Fe_3O_4 MNPs) was synthesized using a previously reported chemical coprecipitation method (Zhou et al., 2010). In brief, 50 mL aqueous solution containing fulvic acid (2 mmol) was purged with argon to remove oxygen and then heated to reflux (101 °C). Then, 4 mL diluted HCl solution containing 2 mmol $FeCl_3 \cdot 6H_2O$ and 1 mmol $FeSO_4 \cdot 7H_2O$ was injected into the hot solution rapidly, followed by concentrated ammonia solution (25 mL). The mixture was kept refluxing for 2 h and then cooled to room temperature. The products were collected after centrifugation and washed four times with ultrapure water and dispersed in ultrapure water. The water-soluble carboxyl-Fe_3O_4 MNPs was obtained. The original concentration of carboxyl-Fe_3O_4 MNP analyzed by ICP was 7.14 mg/mL, which would be used to prepare other concentrations of carboxyl-Fe_3O_4 MNP solution by dilution and stored at 4 °C.

For optimizing concentration of Ab combined with carboxyl-Fe_3O_4 MNPs, BSA was used as the control sample according to the previous reported method (Zhao et al., 2009). The Ab was conjugated

to carboxyl-Fe_3O_4 MNP using EDC/NHS coupling procedure (Zou et al., 2008; Wang et al., 2009). In brief, the carboxyl-Fe_3O_4 MNPs were diluted into pH 7.4 PBS buffer with a final concentration of 0.446 mg/mL. The 400 μL EDC/NHS (0.4 M/0.1 M in PBS buffer) were added to 200 μL of carboxyl-Fe_3O_4 MNPs solution under stirring for 7 min, and sonicated for 5 min in an ice bath to activate the carboxyl group on the surface of Fe_3O_4 MNPs. After that, 200 μL of 0.27 mg/mL Ab was added in this solution under gentle shaking for 10 min, and the solution was sonicated for 5 min in an ice bath to immobilize Ab on the surface of Fe_3O_4 MNPs. And then, 200 μL EA was added for 5 min with vortex shaking at room temperature, and this solution was incubated at 4 °C for 30 min to block all non-specific binding sites. After separation with a magnet and washing twice with PBS buffer, the Fe_3O_4 MNPs of biofunctionalization were dispersed in PBS buffer and stored at 4 °C and it can keep the Ab activity for at least two months. The molarity ratio of Ab-to-Fe_3O_4 MNPs was estimated at 10:1.

2.4. In situ SPR measurement

Scheme S1 is a schematic illustration of the detection principle of the Fe_3O_4 MNPs enhanced SPR sensor for deltamethrin. Initially, to eliminate any possible contamination on the surface of the bare Au chip, the bare Au chip was immersed into the anhydrous ethanol for 5 min. After repeatedly washing with ultrapure water, the Au chip was thoroughly dried with N_2 and was annealed in a hydrogen flame. Then cleaned Au chip placed on the prism with the index-matching oil and covered with the cuvette. After the stable baseline being obtained, 50 μL of a freshly prepared 0.4 mg/mL MEA solution (dissolved with PBS buffer) was injected into SPR cell at 5 μL/min. Upon formation of the MEA self-assembled monolayers (SAMs), the surface of the sensor chip was rinsed with PBS buffer in order to clean out non-specific adsorption. Next, 50 μL chitosan solution was injected into SPR cell at 10 μL/min. Due to adsorption of chitosan viscosity and the interaction between the amino (NH_2) groups of MEA and the hydroxy (OH) groups of chitosan, the chitosan were immobilized on the sensor chip (Kaushik et al., 2009).

The amplification of deltamethrin detection was conducted in the form of a direct assay using the Fe_3O_4 MNP–Ab–deltamethrin conjugates. The detection procedure is made up of two steps. First, Fe_3O_4 MNP–Ab conjugates solution was mixed with different concentration of deltamethrin for 30 min, respectively. After that, deltamethrin bound with Fe_3O_4 MNP–Ab conjugates were separated using a magnet, as illustrated in Scheme S1A. The precipitation was dispersed in PBS again. Second, the resulting solution was injected into the SPR cell at 10 μL/min. The deltamethrin was directly detected by SPR sensor due to the interaction between the amino (NH_2) groups of chitosan and carbonium ion of the deltamethrin (Kaushik et al., 2009). The surface of the SPR chip can be regenerated using acetic acid buffer of pH 5.4 after each binding cycle. To confirm the reproducibility of the detection result, the deltamethrin with different concentrations are repeatedly detected for three times. A calibration plot with linear regression of the relative response against deltamethrin concentration was plotted. To further demonstrate the amplification effect of Fe_3O_4 MNPs, direct detection format without Fe_3O_4 MNP label was implemented via antibody–antigen recognition.

2.5. Analysis of soybean samples

The fresh soybean were kept in oven for 12 h in 60 °C. The dried soybeans were smashed and sieved (100 meshes). Then soybean sample (0.1 g) was extracted with 10 mL of 80% (v/v) methanol for 30 min using an automatic shaker. The crude extract was centrifuged at 10,000 rpm for 10 min. The supernatant was then diluted by PBS. All samples were passed through a 0.2 μm filter before being used in all measurements. During recovery tests, several standard levels were spiked to blank soybean samples. To validate the SPR sensor performance, samples and recovery were analyzed with both the SPR sensor and GC-ECD method.

2.6. GC analysis

GC analysis was performed as follows. In brief, 10 g sample were extracted with 20 ml petroleum ether for 30 min using an automatic shaker. Then crude extract was centrifuged at 4500 rpm for 5 min. After filtration, 2 mL extract was added to activated cartridge of the Agela Cleanert Florisil-SPE, and was eluted with 100 mL mix solution of the petroleum ether–ethyl acetate (95+5, v/v). The extract was evaporated at room temperature and reconstituted in 1 mL of n-hexane. The stock solution of deltamethrin was prepared by dissolving the pure deltamethrin in n-hexane.

GC analyses were run on a Agilent 6890 Series GC chromatograph (Agilent 6890A, USA) with the two same ECDs and two capillary columns, which were a 30 m × 0.25 mm × 0.25 μm DB-17MS capillary column (Aglient Technologies, Inc. 122-4732, USA) for qualitative illustration and a 30 m × 0.25 mm × 0.25 μm HP-1 capillary column (Aglient Technologies, Inc.190912-433, USA) for quantitative determination, respectively. The nitrogen was maintained at a flow rate of 64.4 mL/min to be the carrier gas. The column was programmed as follows: 180 °C for 5 min, directly to 230 °C at 5 °C/min and holding for 10 min, then directly to 280 °Cat 5 °C/min and holding for 20 min. The injector port was maintained at 250 °C and 1 μL sample volume was injected in split mode, and detector temperature was maintained at 300 °C. The split ratio of the front column and back column is 1.3:1 and 50:1, respectively. The total analysis time was 50 min.

3. Results and discussion

3.1. Characterization of functionalized Fe_3O_4 MNPs

The essential prerequisite for proposed approach is to prepare Fe_3O_4 MNP–Ab conjugates. For this purpose, EDC and NHS are used as a carboxyl activating agent for the coupling of primary amines in Ab and carboxyl groups in Fe_3O_4 MNPs. To demonstrate that MNPs have been labeled by Ab successfully, the morphology and structure of the synthesized Fe_3O_4 MNPs and Fe_3O_4 MNP–Ab conjugates were examined using TEM (Fig. S1A and B). It is clearly observed that Fe_3O_4 MNPs and Fe_3O_4 MNP–Ab conjugates were fine, with an average diameter of 6.53 ± 0.22 nm and 9.12 ± 0.63 nm (Fig. S1C, $n=300$ particles). The cluster-like structure of the particles may be resulted from the adsorption of molecules from the surroundings onto the surface to achieve inter-molecular force equilibrium (Baraton et al., 1996). The conjugates increased thickness was consistent with the previous report (Xu et al., 2011). Fe_3O_4 MNP–Ab conjugates show a good stability in the PBS buffer, which are beneficial for the acquisition of accurate and repeated SPR analytical results.

Fig. S1D shows the UV–vis spectra of the Ab, Fe_3O_4 MNPs, and Fe_3O_4 MNP–Ab conjugates. There is an obvious absorption band at 255–290 nm in the spectra of Ab. However, a broad absorption band at 245–265 nm is clearly observed in the spectrum of Fe_3O_4 MNP–Ab. This may be attributed to the formation of complex between Ab and Fe_3O_4 MNPs. The shift of the absorption peak originates primarily from the light absorption and scattering of Fe_3O_4 MNPs, and is the characteristic of semiconductors with indirect band gap (Kaushik et al., 2008; Zhao et al. 2006). This suggests the successful immobilization of Ab on the Fe_3O_4 MNPs surface.

The FT-IR spectra of Fe_3O_4 MNPs and Fe_3O_4 MNP–Ab conjugates are shown in Fig. S1E. As shown in Fig. S1E, the FT-IR spectrum of carboxyl-Fe_3O_4 MNP exhibits a typical Fe–O–Fe absorption bands at 548 cm^{-1}, and the C=O and O–H stretches of the COOH at ~1710 cm^{-1} and ~3500 cm^{-1} (Wang et al., 2010), which indicates

the fulvic acid was chemical bound on the surface of the Fe_3O_4 MNP. Comparing with the FT-IR spectra of carboxyl-Fe_3O_4 MNP, the characteristic peaks of N–H of the CONH at 3100–3600 cm^{-1} were observed in the FT-IR spectrum of Fe_3O_4 MNP–Ab. Therefore, Ab is believed to coat on the surface of Fe_3O_4 MNP by CONH formed through reaction between $–NH_2$ of the Ab and –COOH of the Fe_3O_4 MNP.

3.2. SPR response and concentration dependence of Fe_3O_4 MNPs

The concentration of Fe_3O_4 MNPs plays an important role in our experiments. On the one hand, the using of excessively high concentration Fe_3O_4 MNPs would probably result in the blocking of SPR sensor pipeline (0.01 in. diameter). Additionally, the surface area of the sensor is definite, which limits the maximum amount of Fe_3O_4–Ab conjugates immobilized on the sensor surface. So, the excessively high concentration Fe_3O_4 MNPs would also cause the waste of Ab. On the other hand, excessively low concentration of MNPs would not probably induce enough SPR response for detecting of traces deltamethrin. So, the dependence of SPR response on Fe_3O_4 MNPs concentration was studied (Fig. S2). MEA is used on SPR Au chip for the adsorption of Fe_3O_4 MNPs. The thiol group binds to the Au surface, leaving the amine group to bind with carboxyl group in soluble Fe_3O_4 MNPs by electrostatic interaction. When Fe_3O_4 MNPs concentration was less than 0.89 mg/mL, the SPR response gradually increased with the increase of Fe_3O_4 MNPs concentration, while the further increasing Fe_3O_4 MNPs concentration resulted in a decrease of the SPR response. This is possibly ascribed to Fe_3O_4 MNPs arranged randomly due to steric crowding rather than monolayer self-assembly on the chip surface when using excessively high concentration Fe_3O_4 MNPs, which results in MNPs accumulation on the chip surface. Consequently, after the chip surface being rinsed by PBS buffer to achieve kinetics equilibrium of the association and dissociation between MNPs and chip surface, a lower immobilization density of MNPs will be obtained. Considering the increase of conjugates size caused by Ab being conjugated to Fe_3O_4 MNPs (Fe_3O_4 MNPs (6.53 ± 0.22 nm), Fe_3O_4 MNPs–Ab conjugates (9.12 ± 0.63 nm)) and 95.67% of the coverage $((\Delta RU)/(\Delta RU_{max}))=0.9567$) obtained for 0.446 mg/mL Fe_3O_4 MNPs, the concentration of 0.446 mg/mL will be used in our experiment.

3.3. Preparation of the chip surface

At first, Fe_3O_4 MNP–Ab–deltamethrin conjugates were flowed on the surface of the bare SPR chip to directly detect deltamethrin. However, the result shows there was no SPR response. This demonstrates that Fe_3O_4 MNP–Ab–deltamethrin conjugates cannot be adsorbed or bound on the chip surface. As a result, a linker is required between SPR chip and Fe_3O_4 MNP–Ab–deltamethrin in order to directly detect deltamethrin. Chitosan may act as the linker due to the interaction between the amino (NH_2) groups of chitosan and carbonium ion of the deltamethrin. To select the proper concentration of chitosan so that the compact monomolecular layer can be formed on the chip surface without plugging up the pipeline, a series of chitosan solution of different concentrations (dissolved in 50 mM acetic acid buffer, pH 4.2) was separately injected into the SPR cell. Fig. 1 illustrates the tendency of SPR signal relating to the chitosan concentration. It is found from Fig. 1 that SPR response was about 2050 RU at a chitosan concentration of 1.2 mg/mL, and kept nearly constant for the further increase of chitosan concentration. Considering the viscosity of chitosan, the immobilized chitosan concentration of 1.2 mg/mL was chosen for the subsequent assays.

3.4. Fe_3O_4 MNPs enhanced SPR sensing for the detection of deltamethrin

The amplification level provided by the Fe_3O_4 MNPs was demonstrated by two separate deltamethrin detection formats: (a) direct

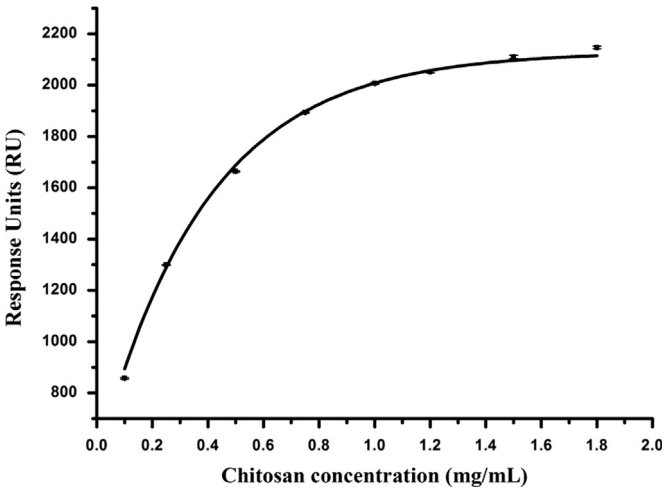

Fig. 1. SPR response graph for chitosan of different concentrations immobilized onto sensor chip surface modified with MEA. And the relative standard deviation range was 0.13–0.40%. The effective stability of the chitosan immobilized chip surface was estimated by rushing with PBS for 30 min.

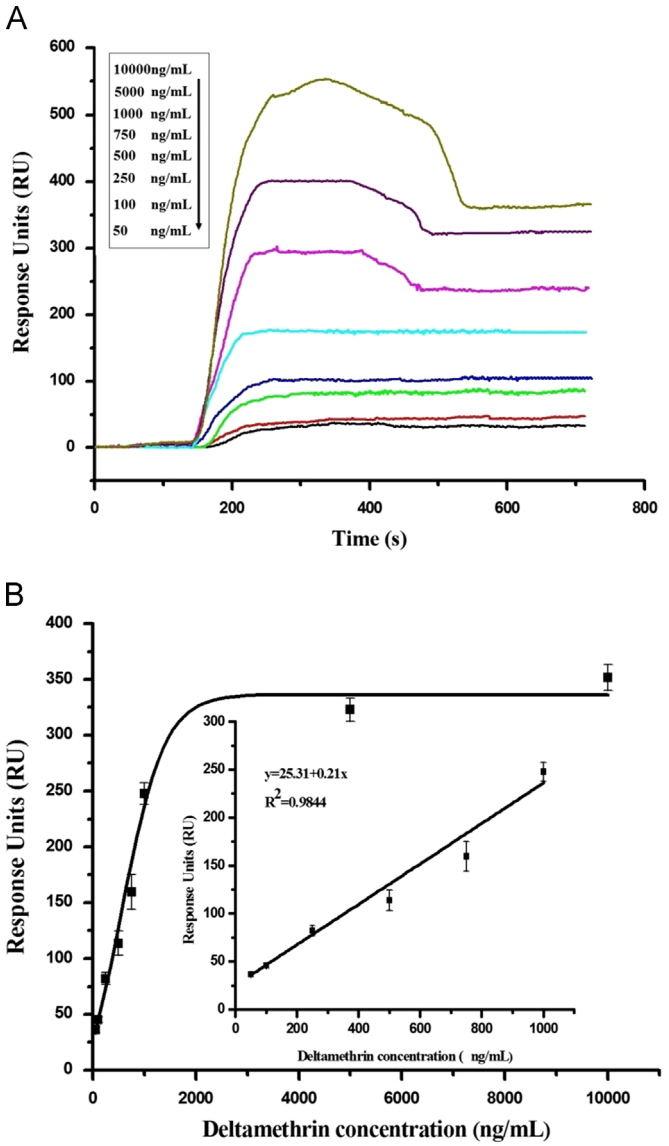

Fig. 2. SPR sensorgram and calibration curve of detection deltamethrin for direct detection format (A and B).

detection format via antibody–antigen recognition without Fe_3O_4 MNPs; (b) amplification detection format with Fe_3O_4 MNP–Ab conjugates. For the direct detection format, through standard amine coupling method, Ab was immobilized onto the sensor surface modified with MPA. After SPR baseline being kept constant caused by the chip surface being rinsed with PBS buffer, 50 μL of EA (0.1 M, in PBS buffer) was injected into the SPR cell at 10 μL/min for 10 min to block unreacted sites on the sensor surface. Subsequently, a series of deltamethrin solution with different concentration was separately injected into the SPR cell, followed by being rinsed with PBS. Meanwhile, the optimal concentration of Ab immobilized on the sensor surface had been first determined to be 0.25 mg/mL. Fig. 2A shows the representative real-time sensorgram of SPR for detection of deltamethrin with direct detection format. It can be clearly seen from Fig. 2A that the SPR responses gradually increase with the deltamethrin concentration increasing from 50 to 10,000 ng/mL. However, when deltamethrin concentration is lower than 50 ng/mL (SPR response is 36.59 RU), it is very difficult to discriminate the concentration of deltamethrin by SPR spectroscopy. While the further increasing of deltamethrin concentration to 10,000 ng/mL resulted in a larger SPR response (351.82 RU), the sensor chip surface has been almost entirely covered by deltamethrin (Fig. 2B). A good linear relationship was obtained between SPR responses and deltamethrin concentrations from 50 ng/mL to 1000 ng/mL (inset in Fig. 2B), and concentrations as low as 50 ng/mL can be readily measured. The relative standard deviation (RSD) range is 3.22–9.69%. The regression equation was $Y=25.31+0.21\times X$ ($R^2=0.9844$, here, X is the concentration of deltamethrin (ng/mL) and Y is the SPR response (RU)).

For amplification detection format, the performance of the Fe_3O_4 MNPs enhanced SPR sensing was evaluated by detecting Fe_3O_4 MNP–Ab–deltamethrin standard solution. After the separation and enrichment with a magnet, 50 μL of Fe_3O_4–Ab–deltamethrin complexes with various deltamethrin concentrations (0–25 ng/mL) were injected into the SPR sell, successively. The in situ SPR curve and the calibration curve of the deltamethrin detection are shown in Fig. 3A and B. As seen from Fig. 3A, the SPR response resulted from the binding of Fe_3O_4–Ab–deltamethrin conjugates gradually increased with increasing deltamethrin concentration, which enables us to detect the trace deltamethrin. It should be pointed out that the SPR response is 6.47 RU (RSD 3.30%) when the Fe_3O_4–Ab conjugates were

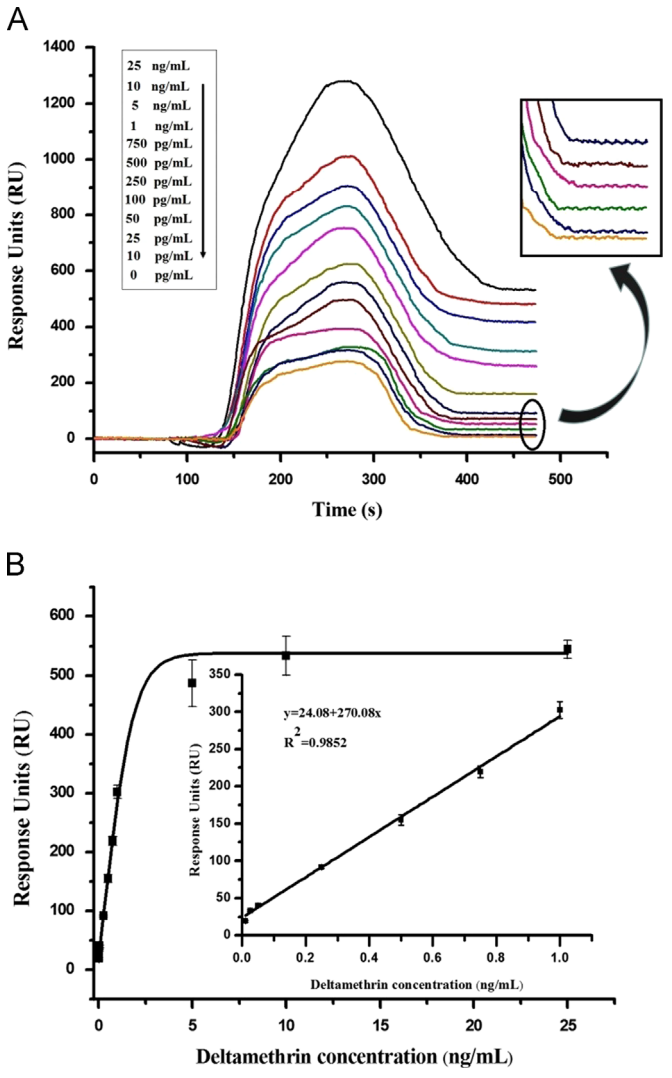

Fig. 3. SPR sensorgram and calibration curve of detection deltamethrin for Fe_3O_4 MNPs enhanced detection format (A and B).

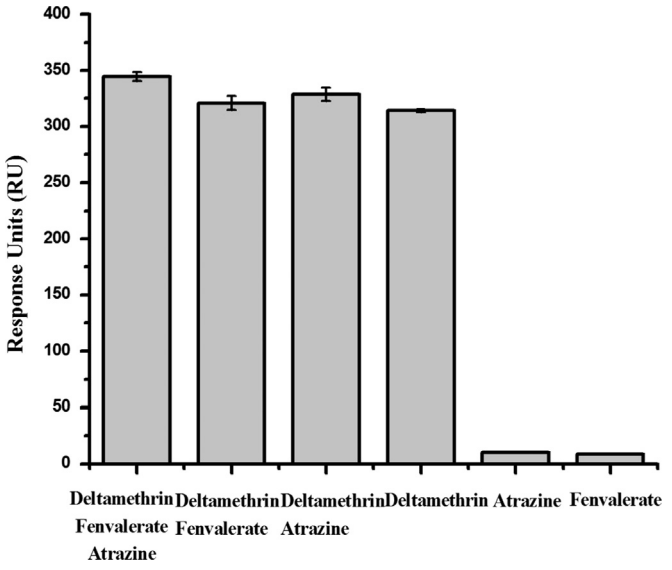

Fig. 4. Specificity analysis of Fe_3O_4 MNPs enhanced SPR detection. Concentrations of deltamethrin, fenvalerate and atrazine were in the same concentration of 1 ng/mL.

Table 1
Comparison with other reported methods for the detection of deltamethrin.

Analytical technique	Concentration range	Detection limit	Ref.
Fluorescence sensor based on CdTe quantum dots and highly fluorescent silica molecularly imprinted nanospheres embedded CdTe QDs	0.5-35.0 μg/mL	0.16 μg/mL	Ge et al. (2011a)
Chemiluminescence sensor based on CdTe quantum dots and deltamethrin imprinted polymers by layer-by-layer (LBL) assembly	0.053-46.5 μg/mL	0.018 μg/mL	Ge et al. (2011b)
Impedance spectroscopy format based on interdigital gold sensor via LBL films of PAH and PAZO	0.01-1 ng/mL	Below 0.01 ng/mL	Abegão et al. (2013)
SPR sensor based on antibody-antigen recognization in direct format	50-1000 ng/mL	Below 50 ng/mL	This work
SPR sensor based on MNPs enhancement format	0.01-1 ng/mL	Below 0.01 ng/mL	This work

Table 2
Recovery test results for spiked soybean samples.

Sample	MNPs enhanced format				Direct format				GC-ECD format			
	Amount spiked (pg/mL)	Amount measured[a] (pg/mL)	Recovery (%)	RSD (%)	Amount spiked (ng/mL)	Amount measured[a] (ng/mL)	Recovery (%)	RSD (%)	Amount spiked (ng/mL)	Amount measured[a] (ng/mL)	Recovery (%)	RSD (%)
1	250	258.99	103.6	13.72	250	203.25	81.3	6.7	250	221.86	88.74	5.13
2	500	522.12	104.4	2.18	500	383.19	76.6	4.37	500	414.47	82.89	8.28
3	750	727.08	96.94	4.35	750	695.45	92.7	3.99	750	632.65	84.35	9.65

[a] Mean values of three determinations.

injected into the SPR cell without deltamethrin. This is probably due to nonspecific adsorption effect of Ab. The 0.01 ng/mL deltamethrin induces SPR response of 19.34 RU. While the 25 ng/mL deltamethrin results in a larger SPR response (545.43 RU). It may be obviously seen from Figs. 3B and 2B that the sensor response saturation for amplification detection format occurs at much lower deltamethrin levels than direct detection format. This enhancement is due to the larger mass and higher refractive index of the Fe_3O_4.

A good linear relationship was obtained between SPR responses and deltamethrin concentrations over a range of 0.01–1 ng/mL (inset in Fig. 3B). The deltamethrin concentrations as low as 0.01 ng/mL can be readily measured, which is more than 4 orders of magnitude lower than that by direct detection format (50 ng/mL) and GC-ECD method (0.1 ug/mL). The RSD range is 1.69–8.10%. The regression equation was $Y=24.08+270.08\times X$ ($R^2=0.9852$). As shown in Table 1, comparing with other sensors for the deltamethrin detection, the presented approach has the lowest detection limit.

3.5. Selectivity

To evaluate the selectivity of the amplification detection format with Fe_3O_4 MNP–Ab conjugates, deltamethrin (1 ng/mL), two different pesticides (1 ng/mL) including fenvalerate, atrazine, the mixture of deltamethrin (1 ng/mL) and each of the pesticides (1 ng/mL), and deltamethrin solution containing two pesticides were measured using the amplification detection format, respectively. The results are shown in Fig. 4, from which it can be observed that deltamethrin has an average response of 314 RU which was much greater than that of the other pesticides (10 RU). In addition, similar SPR responses were obtained for deltamethrin detection in three mixed samples. These results confirm that the proposed SPR approach has a sufficient specificity for deltamethrin detection.

3.6. Real sample analysis

In order to prove the applicability of this SPR signal enhancement strategy to real world samples, soybean sample were spiked with deltamethrin by standard addition method. Recovery tests were separately performed for deltamethrin using the amplification detection format, direct detection format and GC-ECD method. The blank soybean samples were analyzed by GC-ECD to confirm that they do not contain deltamethrin. The experimental results were listed in Table 2. Comparing with direct detection format and GC-ECD, the relative good recovery (96.94–104.4%) and RSD (2.18–13.72%) for trace deltamethrin were obtained using the amplification detection format. The results imply that this proposed SPR approach has high accuracy and is feasible for determining deltamethrin in real sample.

4. Conclusions

In summary, a novel MNPs enhanced SPR sensor for specific and quantitative detection of deltamethrin with low interference and high sensitivity has been constructed. Meanwhile, Fe_3O_4 MNPs not only has been exhibited excellent capability of amplification SPR signal, which resulted in a high sensitivity for the deltamethrin detection, but also excellent extracting and separating capability, which resulted in a high accuracy for the deltamethrin detection in complex agriculture products. The present study demonstrated a presumable general way, and thus will be a simple strategy for the direct detection of various small molecules of interest by altering the type of biomolecule used to label MNPs.

Acknowledgements

This work was financially supported by the National Natural Science Foundation of China (No. 31201375) and Special Fund for Agro-Scientific Research in the public interest (No. 201303084).

Appendix A. Supporting information

Supplementary data associated with this article can be found in the online version at http://dx.doi.org/10.1016/j.bios.2014.03.020.

Reference

Abegão, L.M.G, Ribeiro, J.H.F., Ribeiro, P.A., Raposo, M., 2013. Sensors 13, 10167–10176.
Baraton, M.I., Chen, X., Gonsalves, K.E., 1996. In: Chow, G.M., Gonsalves, K.E. (Eds.), Nanotechnology Molecularly Designed Materials, 1st ed. American Chemical Society, Washington DC, p. 313.
Beccati, D., Halkes, K.M., Batema, G.D., Guillena, G., Souza, A.C., Koten, G.V., Kamerling, J.P., 2005. Chem. Bio. Chem. 6 (7), 1196–1203.
Chang, C.C., Lin, S., Wei, S.C., Chen, C.Y., Lin, C.W., 2011. Biosens. Bioelectron. 30 (1), 235–240.
Chen, H.W., Medley, C.D., Sefah, K., Shangguan, D., Tang, Z.W., Meng, L., Smith, J.E., Tan, W.H., 2008. Chem. Med. Chem. 3 (6), 991–1001.
Ding, H.Y., Bao, X.X., Zheng, Z.Q., 2000. J. Instrum. Anal. 19, 31–34.
Elliot, M., Farnham, A.W., Janes, N.F., Needham, P.H., Pulman, D.A., 1974. Nature 248 (5450), 710–711.
Esteve-Turrillas, F.A., Pastor, A., Guardia, M.D.L., 2005. Anal. Chim. Acta 553 (1−2), 50–57.
Ferrer, C., Gomez, M.J., Garcia-Reyes, J.F., Ferrer, I., Thurman, E.M., Alba, A.R.F., 2005. J. Chromatogr. A 1069 (2), 183–194.
Ge, S.G., Lu, J.J., Ge, L., Yan, M., Yu, J.H., 2011a. Spectrochim. Acta, Part A 79 (5), 1704–1709.
Ge, S.G., Zhang, C.C., Yu, F., Yan, M., Yu, J.H., 2011b. Sens. Actuators, B 156 (1), 222–227.
Gorge, G., Nagel, R., 1990. Ecotoxicol. Environ. Saf. 20 (3), 246–255.
Heidari, H., Razmi, H., Jouyban, A., 2012. J. Chromatogr. A 1245, 1–7.
Kaushik, A., Khan, R., Solanki, P.R., Pandey, P., Alam, J., Ahmad, S., Malhotra, B.D., 2008. Biosens. Bioelectron. 24 (4), 676–683.
Kaushik, A., Solanki, P.R., Ansari, A.A., Malhotra, B.D., Ahmad, S., 2009. Biochem. Eng. J. 46 (2), 132–140.
Kim, E.J., Chung, B.H., Lee, H.J., 2012. Anal. Chem. 84 (22), 10091–10096.
Koprücü, K., Aydın, R., 2004. Pestic. Biochem. Physiol. 80 (1), 47–53.
Liang, R.P., Yao, G.H., Fan, L.X., Qiu, J.D., 2012. Anal. Chim. Acta 737, 22–28.
Lin, K.Q., Lu, Y.H., Chen, J.X., Zheng, R.S., Wang, P., Ming, H., 2008. Opt. Express 16 (23), 18599–18604.
Luckarift, H.R., Balasubramanian, S., Paliwal, S., Johnson, G.R., Simonian, A.L., 2007. Colloids Surf., B 58 (1), 28–33.
Pelossof, G., Tel-Vered, R., Willner, I., 2012. Anal. Chem. 84 (2), 3703–3709.
Ray, D.E., Ray, D., Forshaw, P.J., 2000. Clin. Toxicol. 38 (2), 95–101.

Tsochatzis, E.D., Menkissoglu-Spiroudi, U., Karpouzas, D.G., Tzimou-Tsitouridou, R., 2010. Anal. Bioanal. Chem. 397 (6), 2181–2190.
Urusov, A.E., Kostenko, S.N., Sveshnikob, P.G., Zherdev, A.V., Dzantiev, B.B., 2011. Sens. Actuators, B 156 (1), 343–349.
Vasileva, P., Donkova, B., Karadjova, I., Dushkin, C., 2011. Colloids Surf., A 382 (1–3), 203–210.
Velíšek, J., Jurčíková, J., Dobšíková, R., Svobodová, Z., Piačková, V., Máchová, J., Novotný, L., 2007. Environ. Toxicol. Pharmacol. 23 (3), 297–301.
Vázquez, P.P., Mughari, A.R., Martinez, G.M., 2008. Anal. Chim. Acta 607 (1), 74–82.
Wang, J.L., Munir, A., Zhu, Z.Z., Zhou, H.S., 2010. Anal. Chem. 82 (16), 6782–6789.
Wang, J.L., Zhu, Z.Z., Munir, A., Zhou, H.S., 2011. Talanta 84 (3), 783–788.
Wang, J.Y., Wang, Q., Ren, L., Wang, X.Q., Wan, Z.F., Liu, W.M., Li, L., Zhao, H.Y., Li, M.L., Tong, D.W., Xu, J., 2009. Colloids Surf., B 72 (1), 112–120.
Wang, Y., Dostalek, J., Knoll, W., 2011. Anal. Chem. 83 (16), 6202–6207.
Wongsa, N., Burakham, R., 2012. Food Anal. Method 5 (4), 849–855.
Xu, H.Y., Aguilar, Z.P., Yang, L., Kuang, M., Duan, H.W., Xiong, Y.H., Wei, H., Wang, A., 2011. Biomaterials 32 (36), 9758–9765.
Zamfir, L.G., Geana, I., Bouriguac, S., Rotariu, L., Bala, C., Errachid, A., Jaffrezic-Renault, N., 2011. Sens. Actuators, B 159 (1), 178–184.
Zhao, G., Xu, J.J., Chen, H.Y., 2006. Electrochem. Commun. 8 (1), 148–154.
Zhao, Y., Ye, M.Q., Chao, Q.G., Jia, N.Q., Ge, Y., Shen, H.B., 2009. J. Agric. Food Chem. 57 (2), 517–524.
Zhou, C.J., Rong, P.F., Zhang, W.J., Zhou, J.D., Zhang, Q.L., Wang, W., Zou, B.S., 2010. Funct. Mater. Lett. 3 (3), 197–200.
Zou, M.Q., Gao, H.X., Li, J.F., Xu, F., Wang, L., Jiang, J.Z., 2008. Anal. Biochem. 374 (2), 318–324.